8-2016

Right-Hand Polarized $4f_{ce}$ Auroral Roar Emissions: 2. Nonlinear Generation Theory

P. H. Yoon

J. LaBelle

Allan T. Weatherwax
Merrimack College, weatherwaxa@merrimack.edu

AGU PUBLICATIONS

JGR

Journal of Geophysical Research: Space Physics

RESEARCH ARTICLE

10.1002/2016JA022889

This article is a companion to *LaBelle and Chen* [2016], doi:10.1002/2016JA022890.

Key Points:

- Nonlinear theory for $4f_{ce}$ roar is proposed
- Two upper hybrid or *Z* modes merge to emit *X* mode radiation
- Theory explains observed $4f_{ce}$ roars

Correspondence to:
P. H. Yoon,
yoonp@umd.edu

Citation:
Yoon, P. H., J. LaBelle, and A. T. Weatherwax (2016), Right-hand polarized $4f_{ce}$ auroral roar emissions: 2. Nonlinear generation theory, *J. Geophys. Res. Space Physics*, *121*, 7981–7987, doi:10.1002/2016JA022889.

Received 29 APR 2016
Accepted 6 JUL 2016
Accepted article online 12 JUL 2016
Published online 13 AUG 2016

Right-hand polarized $4f_{ce}$ auroral roar emissions: 2. Nonlinear generation theory

P. H. Yoon[1,2], J. LaBelle[3], and A. T. Weatherwax[4]

[1]Institute for Physical Science and Technology, University of Maryland, College Park, Maryland, USA, [2]School of Space Research, Kyung Hee University, Yongin-Si, Gyeonggi-Do, Korea, [3]Department of Physics and Astronomy, Dartmouth College, Hanover, New Hampshire, USA, [4]School of Science and Engineering, Merrimack College, North Andover, Massachusetts, USA

Abstract Auroral roar emissions are commonly interpreted as *Z* (or upper hybrid) mode naturally excited by precipitating auroral electrons. Subsequent conversion to escaping radiation makes it possible for these emissions to be detected on the ground. Most emissions are detected as having left-hand (*L*) circular (or ordinary *O*) polarization, but the companion paper presents a systematic experimental study on the rare occurrence of the right-hand polarized, or equivalently, extraordinary (*X*) mode $4f_{ce}$ emission. A similar observation was reported earlier by Sato et al. (2015). The suggested emission mechanism is the nonlinear coalescence of two upper hybrid roars at $2f_{ce}$. The present paper formulates a detailed theory for such an emission mechanism.

1. Introduction

The auroral roar emission is a megahertz range narrowband radiation detected on the ground in the Earth's auroral zone. The auroral roar was first discovered at $2f_{ce}$ [*Kellogg and Monson*, 1979], where $f_{ce} = \Omega_e/(2\pi)$ stands for electron cyclotron frequency and $\Omega_e = eB_0/m_ec$ being the angular electron gyrofrequency. Here e, B_0, m_e, and c stand for unit electric charge, ambient magnetic field intensity, electron mass, and the speed of light, respectively. Subsequently, $3f_{ce}$ roar was discovered [*Weatherwax et al.*, 1993]. The general understanding of the emission mechanism is based on the relativistic cyclotron maser type of resonant instability of *Z* mode waves excited by the precipitating auroral electrons possessing a horseshoe (or generalized loss cone) momentum distribution function [*Yoon et al.*, 1998]. The *Z* or upper hybrid wave growth is enhanced when the local upper hybrid frequency matches twice or thrice the local electron cyclotron frequency, $f_{\rm uh} \approx nf_{ce}$, for $n = 2, 3$, a condition that can be satisfied near the *F* region peak ionospheric altitude at nighttime. Here the upper hybrid frequency $f_{\rm uh}$ is defined by $f_{\rm uh}^2 = f_{ce}^2 + f_{pe}^2$, where $f_{pe} = \omega_{pe}/(2\pi)$ is the electron plasma frequency and $\omega_{pe} = (4\pi n_0 e^2/m_e)^{1/2}$ is the angular frequency. The quantity n_0 represents the ambient electron density.

The ground-level detection of the auroral roar is believed to be the result of mode conversion of upper hybrid/*Z* mode to left-hand/*O* mode at the density gradient. Indeed, the measured polarization of $2f_{ce}$ and $3f_{ce}$ is consistent with this interpretation in that the *L*-*O* mode polarization is dominant for these emissions [*Shepherd et al.*, 1997; *Sato et al.*, 2008]. Recently, $4f_{ce}$ [*Sato et al.*, 2012] and $5f_{ce}$ [*LaBelle*, 2012; *LaBelle and Dundek*, 2015] auroral roars have also been detected near the sunlit side of the ionosphere where the electron density is enhanced via photoionization.

In a recent paper, *Sato et al.* [2015] reported the first polarization measurements of $4f_{ce}$ auroral roars. According to their study, while the majority of $4f_{ce}$ roars detected under the sunlit condition are polarized in the sense of left-hand/*O* mode, thus supporting the direct linear mode conversion paradigm, a couple of intriguing right-hand/*X* mode polarized $4f_{ce}$ roars under darkness was also observed. The authors suggest that these roars are the consequence of two upper hybrid or *Z* mode roars at $2f_{ce}$ nonlinearly coupling to produce the *X* mode at twice their frequencies. *Sato et al.* [2010] also proposed the same mechanism to interpret the anomalous polarization from the topside ionosphere.

A companion paper [*LaBelle and Chen*, 2016] reports the result of a systematic study at Sondrestrom, Greenland, of all $4f_{ce}$ auroral roar emissions detected by a dedicated experiment designed for optimal sensitivity to higher harmonic emissions including polarization measurements. The details of experiment can be found in that paper, but to summarize the findings, the occurrence of $4f_{ce}$ roar emissions increases under sunlit conditions, but every single observation is left-hand polarized. Rare $4f_{ce}$ roars with opposite polarization (right-hand/*X* mode) are detected during nighttime, which is consistent with the earlier report by *Sato et al.* [2015] and suggests the rarity of right-hand polarized (or *X* mode) $4f_{ce}$ roars. It also points to the fact that the emission mechanism for right-hand/*X* mode $4f_{ce}$ roars must be fundamentally different than the customary left-hand/*O* mode polarized roars. In agreement with Sato et al.'s suggestion, we also believe that the most plausible mechanism is the merging of two $2f_{ce}$ roars. The purpose of the present Letter is to quantitatively analyze the nonlinear coalescence emission process by making use of the recently formulated weak turbulence theory for perpendicular propagation [*Yoon*, 2015].

The nonlinear theory of two upper hybrid waves merging to generate the *X* mode radiation actually has been entertained in a variety of contexts before. *Vlahos et al.* [1983] considered such a mechanism for solar microwave bursts. They assumed coherent three-wave interaction, whereas the wave kinetic equation formulated by *Yoon* [2015] is applicable for an incoherent (i.e., broadband in k space) turbulence. *Fung and Papadopoulos* [1987] also considered a similar coherent wave-wave interaction problem to discuss the narrowband Jovian kilometric radiation. *Roux and Pellat* [1979], on the other hand, considered the weak turbulence theory similar to ours, except that their theory is approximate and qualitative. Their theory was an early attempt to explain the auroral kilometric radiation. The works most closely related to the present Letter are those by *Melrose* [1991] and by *Willes et al.* [1998]. *Melrose* [1991] worked out a model of *Z* mode waves undergoing multiple nonlinear coalescence to produce multiple cyclotron harmonic solar spike radio bursts. His theory was adopted by *Willes et al.* [1998] in the context of the auroral roar emission, but *Willes et al.* [1998] were concerned with explaining $2f_{ce}$ and $3f_{ce}$ roars. Because the observed polarization of $2f_{ce}$ and $3f_{ce}$ roars is polarized predominantly in the sense of left-hand/*O* mode, their *Z* mode coalescence theory, which predicts right-hand/*X* mode polarization, did not attract much attention. However, in view of Sato et al.'s and LaBelle et al.'s observation of $4f_{ce}$ right-hand/*X* mode roars, albeit rare in occurrence, it is timely to revisit this mechanism. In the present paper, we make use of recent theory [*Yoon*, 2015] in order to demonstrate that the coalescence of two $2f_{ce}$ upper hybrid/*Z* mode roars is indeed possible. In the remainder of the present paper we discuss the details of our findings.

2. Nonlinear Theory of $4f_{ce}$ Roar

To briefly overview the recent formulation of nonlinear kinetic theory of high-frequency incoherent electromagnetic (EM) perturbations, *Yoon* [2015] considered that the wave vector is assumed to lie in an orthogonal direction, $\mathbf{k} = k\hat{\mathbf{x}}$, with respect to the ambient magnetic field, $\mathbf{B}_0 = B_0\hat{\mathbf{z}}$. With such a simplification, the Vlasov equation was solved in a perturbative way up to the second order in nonlinearity. The nonlinear current is obtained in terms of multiple harmonic series involving the customary Bessel function expansion, which is common to the kinetic theory of magnetized plasmas. By restricting the discussion to magnetoionic modes (i.e., cold-plasma waves) propagating in perpendicular directions, namely, the ordinary EM wave, and two branches (*X* and *Z*) of the extraordinary mode wave, *Yoon* [2015] derived the wave kinetic equation. Yoon's formulation of weak turbulence theory, which is based upon the statistical mechanical approach, is equivalent to the formalism based upon the semi-classical method, as found, e.g., in the paper by *Melrose* [1991].

In the cold limit, it was found that *O* mode does not respond to nonlinear perturbation such that it decouples from *X* and *Z* modes and thus remains in a plane wave state. However, it was also found that *X* and *Z* modes are mutually coupled through nonlinear susceptibility response, and the wave kinetic equations for the two modes are given by

$$\frac{\partial I_\alpha^\sigma(k)}{\partial t} = -\frac{2\pi}{\Lambda'(k,\sigma\omega_k^\alpha)} \sum_{\beta,\gamma=X,Z} \sum_{\sigma',\sigma''=\pm1} \int dk' \left(\frac{a\left(k,k'|\sigma\omega_k^\alpha,\sigma'\omega_{k'}^\beta\right) I_\gamma^{\sigma''}(k-k') I_\alpha^\sigma(k)}{\Lambda'\left(k',\sigma'\omega_{k'}^\beta\right)} + \frac{b\left(k,k'|\sigma\omega_k^\alpha,\sigma'\omega_{k'}^\beta\right) I_\beta^{\sigma'}(k') I_\alpha^\sigma(k)}{\Lambda'\left(k-k',\sigma''\omega_{k-k'}^\gamma\right)} - \frac{c\left(k,k'|\sigma\omega_k^\alpha,\sigma'\omega_{k'}^\beta\right) I_\beta^{\sigma'}(k') I_\gamma^{\sigma''}(k-k')}{\Lambda'\left(k,\sigma\omega_k^\alpha\right)} \right) \times \delta\left(\sigma\omega_k^\alpha - \sigma'\omega_{k'}^\beta - \sigma''\omega_{k-k'}^\gamma\right), \tag{1}$$

where $\alpha = X, Z$ and $\sigma = \pm 1$ signify the direction of wave vector along x axis. The wave electric field intensity, $I_\alpha^\sigma(k)$, for each eigenmode, *X* or *Z*, is related to the total spectral wave electric field energy density by

$|E(k)|^2 = \sum_{\alpha=X,Z} \sum_{\sigma=\pm 1} I_k^{\sigma\alpha} \delta\left(\omega - \sigma\omega_k^\alpha\right)$. Here the linear dispersion relations for X and Z modes are given, respectively, by $\omega = \omega_k^X$ and $\omega = \omega_k^Z$, where

$$\begin{pmatrix} \omega_X^2 \\ \omega_Z^2 \end{pmatrix} = \frac{(\omega_* \pm \Omega_e)^2 - c^4k^4}{4} + c^2k^2. \tag{2}$$

In the above, $\omega_*^2 = \Omega_e^2 + 4\omega_{pe}^2 - 2c^2k^2 + c^4k^4/\Omega_e^2$. In equation (1), the quantity $\Lambda'(k,\omega)$, and the coefficients $a(k,k'|\omega,\omega')$, $b(k,k'|\omega,\omega')$, and $c(k,k'|\omega,\omega')$ represent the derivative of the linear dispersion function and nonlinear mode coupling coefficients, respectively. They are defined by

$$\Lambda'(k,\omega) = \frac{2}{\omega^3} \frac{\omega^2(c^2k^2 + \omega_{\rm uh}^2) - 2c^2k^2\omega_{\rm uh}^2 - \omega_{pe}^4}{\omega^2 - \Omega_e^2}, \tag{3}$$

$$\begin{aligned} a(k,k'|\omega,\omega') = \frac{e^2}{16m_e^2} \frac{\omega_{pe}^4}{\omega\omega'} & \left\{ \sum_{+,-} \frac{1}{\omega \mp \Omega_e} \left(\frac{\omega^2 - \omega_{\rm uh}^2}{\omega^2 - \Omega_e^2} \pm \frac{\Omega_e}{\omega} \frac{\omega_{pe}^2}{\omega^2 - \Omega_e^2} \right) \right. \\ & \times \left(\frac{k'}{\omega'(\omega - \omega' \mp \Omega_e)} + \frac{k - k'}{(\omega - \omega')(\omega' \mp \Omega_e)} \right) \left. \left(1 \pm \frac{\Omega_e}{\omega - \omega'} \frac{\omega_{pe}^2}{(\omega - \omega')^2 - \omega_{\rm uh}^2} \right) \right\} \\ & \times \left\{ \sum_{+,-} \frac{1}{\omega' \mp \Omega_e} \left(\frac{\omega'^2 - \omega_{\rm uh}^2}{\omega'^2 - \Omega_e^2} \pm \frac{\Omega_e}{\omega'} \frac{\omega_{pe}^2}{\omega'^2 - \Omega_e^2} \right) \left(\frac{k - k'}{(\omega - \omega')(\omega \mp \Omega_e)} - \frac{k}{\omega(\omega - \omega' \pm \Omega_e)} \right) \right. \\ & \times \left. \left(2 \pm \frac{\Omega_e}{\omega} \frac{\omega_{pe}^2}{\omega^2 - \omega_{\rm uh}^2} \mp \frac{\Omega_e}{\omega - \omega'} \frac{\omega_{pe}^2}{(\omega - \omega')^2 - \omega_{\rm uh}^2} \right) \right\}, \end{aligned} \tag{4}$$

$$\begin{aligned} b(k,k'|\omega,\omega') = \frac{e^2}{16m_e^2} \frac{\omega_{pe}^4}{\omega(\omega - \omega')} & \left\{ \sum_{+,-} \frac{1}{\omega \mp \Omega_e} \left(\frac{\omega^2 - \omega_{\rm uh}^2}{\omega^2 - \Omega_e^2} \pm \frac{\Omega_e}{\omega} \frac{\omega_{pe}^2}{\omega^2 - \Omega_e^2} \right) \right. \\ & \times \left(\frac{k'}{\omega'(\omega - \omega' \mp \Omega_e)} + \frac{k - k'}{(\omega - \omega')(\omega' \mp \Omega_e)} \right) \left. \left(1 \pm \frac{\Omega_e}{\omega - \omega'} \frac{\omega_{pe}^2}{(\omega - \omega')^2 - \omega_{\rm uh}^2} \right) \right\} \\ & \times \left\{ \sum_{+,-} \frac{1}{\omega - \omega' \mp \Omega_e} \left(\frac{k'}{\omega'(\omega \mp \Omega_e)} - \frac{k}{\omega(\omega' \pm \Omega_e)} \right) \right. \\ & \times \left(\frac{(\omega - \omega')^2 - \omega_{\rm uh}^2}{(\omega - \omega')^2 - \Omega_e^2} \pm \frac{\Omega_e}{\omega - \omega'} \frac{\omega_{pe}^2}{(\omega - \omega')^2 - \Omega_e^2} \right) \\ & \times \left. \left(2 \pm \frac{\Omega_e}{\omega} \frac{\omega_{pe}^2}{\omega^2 - \omega_{\rm uh}^2} \mp \frac{\Omega_e}{\omega'} \frac{\omega_{pe}^2}{\omega'^2 - \omega_{\rm uh}^2} \right) \right\}, \end{aligned} \tag{5}$$

$$\begin{aligned} c(k,k'|\omega,\omega') = \frac{e^2}{16m_e^2} \frac{\omega_{pe}^4}{\omega^2} & \left\{ \sum_{+,-} \frac{1}{\omega \mp \Omega_e} \left(\frac{\omega^2 - \omega_{\rm uh}^2}{\omega^2 - \Omega_e^2} \pm \frac{\Omega_e}{\omega} \frac{\omega_{pe}^2}{\omega^2 - \Omega_e^2} \right) \right. \\ & \times \left(\frac{k'}{\omega'(\omega - \omega' \mp \Omega_e)} + \frac{k - k'}{(\omega - \omega')(\omega' \mp \Omega_e)} \right) \left. \left(1 \pm \frac{\Omega_e}{\omega - \omega'} \frac{\omega_{pe}^2}{(\omega - \omega')^2 - \omega_{\rm uh}^2} \right) \right\} \\ & \times \left\{ \sum_{+,-} \frac{1}{\omega \mp \Omega_e} \left(\frac{\omega^2 - \omega_{\rm uh}^2}{\omega^2 - \Omega_e^2} \pm \frac{\Omega_e}{\omega} \frac{\omega_{pe}^2}{\omega^2 - \Omega_e^2} \right) \left(\frac{k'}{\omega'(\omega - \omega' \mp \Omega_e)} + \frac{k - k'}{(\omega - \omega')(\omega' \mp \Omega_e)} \right) \right. \\ & \times \left. \left(2 \pm \frac{\Omega_e}{\omega'} \frac{\omega_{pe}^2}{\omega'^2 - \omega_{\rm uh}^2} \pm \frac{\Omega_e}{\omega - \omega'} \frac{\omega_{pe}^2}{(\omega - \omega')^2 - \omega_{\rm uh}^2} \right) \right\}. \end{aligned} \tag{6}$$

The detailed derivation of the above result can be found in the paper by *Yoon* [2015].

In what follows, let us consider the situation in which the ratio ω_{pe}/Ω_e is on the order of $\sqrt{3}$ or so, which is the optimal condition for excitation of $2f_{ce}$ upper hybrid/Z mode. Anticipating the final result that the generation of X mode by nonlinear coalescence of two Z modes will occur only over a narrow frequency band around twice the upper hybrid frequency, we may approximate $\omega_X \approx 2\omega_{\rm uh}$ in the nonlinear mode coupling coefficients, a, b, and c, as well as in the factor Λ'. To good approximation, we may also write $\omega_Z \approx \omega_{\rm uh}$. We assume that the wave intensities are symmetric in k so that they do not depend on the index σ. Also, we may choose only +1 signs for the indices σ, σ', and σ''. We assume that the waves are symmetric in k, so we may simply choose $\sigma = 1$ without loss of generality ($\sigma = \pm 1$ represents the direction of wave propagation along k axis). For $\sigma = 1$ and positive real frequencies, only $\sigma' = \sigma'' = 1$ can satisfy the resonance condition, $\sigma\omega_k^\alpha = \sigma'\omega_{k'}^\beta + \sigma''\omega_{k-k'}^\gamma$. Let us also consider a simple situation where the X mode intensity is sufficiently low so that it may be ignored on the right-hand side of equation (1). This approximation leads to substantial simplification of the nonlinear mode coupling coefficients as well as the nonlinear wave kinetic equation. After some manipulations, one can show that the wave kinetic equation for the X mode is approximately given by

$$\frac{\partial I_X(k)}{\partial t} = A\int dk' V_{k,k'} I_Z(k') I_Z(k-k')\delta(\omega_k^X - \omega_{k'}^Z - \omega_{k-k'}^Z), \tag{7}$$

where

$$A = \frac{\pi e^2}{8m_e^2}\frac{\omega_{pe}^4}{\omega_{\rm uh}^2}\frac{\Omega_e^3}{4\omega_{\rm uh}^4 - \omega_{pe}^4 + 2\omega_{\rm uh}^2 c^2 k^2}\left(\sum_{+,-}\frac{6\omega_{\rm uh}^3 \pm \Omega_e\omega_{pe}^2}{(2\omega_{\rm uh} \mp \Omega_e)(\omega_{\rm uh} \mp \Omega_e)}\right),$$

$$\begin{aligned} V_{k,k'} = {} & \frac{\omega_{pe}^2}{\Omega_e}\frac{\omega_{pe}^2 k^2}{(\omega_{k-k'}^Z)^2 - \omega_{\rm uh}^2}\frac{1}{4\omega_{\rm uh}^4 - \omega_{pe}^4 + 2\omega_{\rm uh}^2 c^2 k^2} \\ & \times\left(\frac{1}{(\omega_{k'}^Z)^2 - \omega_{\rm uh}^2} + \frac{1}{(\omega_{k-k'}^Z)^2 - \omega_{\rm uh}^2}\right)\left(\sum_{+,-}\frac{6\omega_{\rm uh}^3 \pm \Omega_e\omega_{pe}^2}{(2\omega_{\rm uh} \mp \Omega_e)(\omega_{\rm uh} \mp \Omega_e)}\right). \end{aligned} \tag{8}$$

In equation (8) the delta-function resonance condition must be computed numerically since closed-form analytical determination of the resonant k' is not forthcoming.

In order to facilitate the analysis, let us introduce dimensionless variables and quantities,

$$\varpi = \frac{\omega}{\Omega_e}, \kappa = \frac{ck}{\Omega_e}, \rho = \frac{\omega_{pe}}{\Omega_e}, \mathcal{I}(\kappa) = \frac{\Omega_e^3}{c^3} I(k). \tag{9}$$

In terms of the above dimensionless quantities, let us also write down the models of X and Z mode dispersion relations,

$$\begin{aligned} \varpi_X(\kappa) &= \sqrt{\varpi_R^2 + \kappa^2}, \\ \varpi_Z(\kappa) &= \frac{\varpi_L + C\varpi_{\rm uh}\kappa^2}{1 + C\kappa^2}, \end{aligned} \tag{10}$$

where $\varpi_{\rm uh} = (1 + \rho^2)^{1/2}$ is the normalized upper hybrid frequency, $\varpi_R = (1/2)[(1 + 4\rho^2)^{1/2} + 1]$ and $\varpi_L = (1/2)[(1 + 4\rho^2)^{1/2} - 1]$ stand for normalized R and L mode cutoff frequencies, respectively, $C = (\varpi_* - \varpi_L)/(\varpi_{\rm uh} - \varpi_*)$, and $\varpi_* = (\varpi_{\rm uh}^2 - \rho)^{1/2}$. Note that model dispersion relations (10) replace the actual dispersion relations (2), but numerical plots of the two formulae show good agreement (not shown). The reason for adopting the model dispersion relations is that they facilitate the numerical root finding scheme in the delta-function resonance condition. In terms of equation (10), the delta-function three-wave resonance condition becomes

$$0 = \varpi_X(\kappa) - \varpi_Z(\kappa') - \varpi_Z(\kappa - \kappa') = \sqrt{\varpi_R^2 + \kappa^2} - \frac{\varpi_L + C\varpi_{\rm uh}\kappa'^2}{1 + C\kappa'^2} - \frac{\varpi_L + C\varpi_{\rm uh}(\kappa - \kappa')^2}{1 + C(\kappa - \kappa')^2}. \tag{11}$$

It turns out that the real root κ' for the above equation exists for κ in the approximate range $2.5 < \kappa < 3.8$ or so. Upon close examination, this range of κ corresponds to $4f_{ce}$ frequency, which shows that the merging of two upper hybrid/Z modes near $2f_{ce}$ is indeed capable of generating X mode at $4f_{ce}$. The range of real roots κ' when κ is limited to the said wave number domain turns out to be roughly $2 < \kappa' < 8$. For such a range of κ', the Z modes $\varpi_Z(\kappa')$ and $\varpi_Z(\kappa - \kappa')$ are characterized by short perpendicular wavelengths such that their frequency is close to the upper hybrid frequency.

In what follows, we simply model the Z mode intensity as a symmetric Gaussian spectrum,

$$\mathcal{I}_Z(\kappa) = \mathcal{I}_0\left[e^{-(\kappa-\kappa_0)^2/\Delta^2} + e^{-(\kappa+\kappa_0)^2/\Delta^2}\right], \tag{12}$$

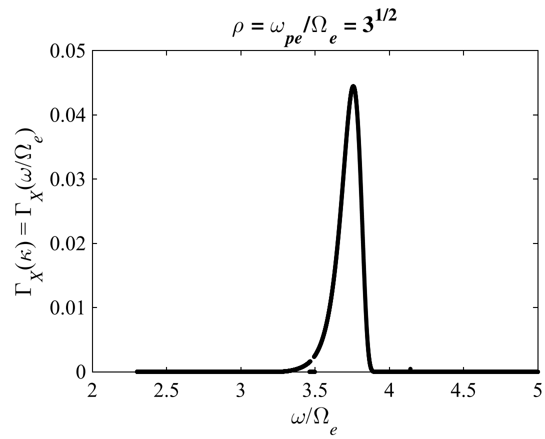

Figure 1. The normalized X mode nonlinear growth rate $\Gamma(\kappa) = \Gamma(\varpi)$ versus $\varpi = \sqrt{\varpi_R + \kappa^2}$ for $\rho = \sqrt{3}$, $\kappa_0 = 4$ and $\Delta = 1$.

where κ_0 and Δ are chosen as $\kappa_0 = 4$ and $\Delta = 1$. We also choose $\rho \sim \sqrt{3}$, which is close to the optimal condition for the matching of upper hybrid frequency and twice the electron cyclotron frequency, $f_{\rm uh} = 2f_{ce}$ (or $\omega_{\rm uh} = 2\Omega_e$). With the above model spectrum for Z mode and the adopted frequency ratio, we define the instantaneous normalized decay instability growth rate for X mode,

$$\Gamma_X(\kappa) \equiv \frac{1}{\Omega_e}\frac{\partial}{\partial t}\frac{\mathcal{I}_X(\kappa)}{\mathcal{I}_0^2} = \frac{\Gamma_0}{\mathcal{I}_0^2} G(\kappa)\mathcal{I}_Z(\kappa_r)\mathcal{I}_Z(\kappa-\kappa_r), \tag{13}$$

where

$$\Gamma_0 = \frac{\pi}{8}\frac{\rho^8}{\varpi_{\rm uh}^2}\frac{\kappa^2}{(4\varpi_{\rm uh}^4 - \rho^4 + 2\varpi_{\rm uh}^2\kappa^2)^2}\left(\frac{6\varpi_{\rm uh}^3+\rho^2}{(2\varpi_{\rm uh}-1)(\varpi_{\rm uh}-1)} + \frac{6\varpi_{\rm uh}^3-\rho^2}{(2\varpi_{\rm uh}+1)(\varpi_{\rm uh}+1)}\right)^2,$$
$$G(\kappa) = \frac{1}{[\varpi_Z(\kappa-\kappa_r)]^2 - \varpi_{\rm uh}^2}\left(\frac{1}{[\varpi_Z(\kappa_r)]^2-\varpi_{\rm uh}^2} + \frac{1}{[\varpi_Z(\kappa-\kappa_r)]^2-\varpi_{\rm uh}^2}\right). \tag{14}$$

In the above, κ_r is the real root of equation (11) determined by a numerical root solving scheme.

Shown in Figure 1 is the normalized X mode nonlinear growth rate $\Gamma(\kappa) = \Gamma(\varpi)$ versus $\varpi = \sqrt{\varpi_R + \kappa^2}$. As Figure 1 indicates, the X mode growth rate is peaked around the frequency range slightly below $4f_{ce}$ in a narrow range occupying frequency bandwidth $\sim 0.1\Omega_e$. This proves that the suggested emission mechanism of two $2f_{ce}$ roars merging to produce $4f_{ce}$ X mode roar [*Sato et al.*, 2010; 2015] may indeed be correct. Note that the normalized nonlinear growth rate depends on a number of unknown quantities such as the Z mode intensities, etc., so that it is difficult to extract actual physical quantities, such as the nonlinear growth time, on the basis of the formal expression. The real purpose is to show the gross property associated with the decay instability that $4f_{ce}$ wave growth does indeed take place.

3. Conclusions and Discussion

In the present paper, a nonlinear decay instability theory for the recently observed $4f_{ce}$ auroral roar with right-hand/X mode polarization [*Sato et al.*, 2015; *LaBelle and Chen*, 2016] is formulated and solved in detail. It is demonstrated that indeed, the upper hybrid/Z mode with twice the electron cyclotron frequency is capable of coalescing in order to produce the fourth-harmonic right-hand/X mode roars.

The Dartmouth College research team have recently completed a survey of all the $4f_{ce}$ roars observed at Sondrestrom facility in which a polarization experiment was installed. The results are discussed in detail in the companion paper [*LaBelle and Chen*, 2016], but briefly, they report that $4f_{ce}$ roars observed under sunlit condition are all left-hand polarized (i.e., O mode), while a couple of $4f_{ce}$ roars at nighttime showed opposite polarization. Such a rarity of right-hand polarized (X mode) $4f_{ce}$ roars is consistent with earlier observation by *Sato et al.* [2015], who reported only two right-hand polarized $4f_{ce}$'s from among 11 events. Note that the Dartmouth research team detected many more events of $4f_{ce}$ roar emissions, yet only two under darkness exhibited the X mode polarization.

In view of this, one may wonder why the nonlinear merging emission is so uncommon. In order to address this issue, we have examined the critical role of input parameters for the nonlinear growth rate (13). There are three basic free parameters. One is the frequency ratio, $\rho = \omega_{pe}/\Omega_e$, but since this ratio determines the excitation of $2f_{ce}$ roars to start with, we do not have much freedom with this parameter. We chose $\rho = \omega_{pe}/\Omega_e \sim \sqrt{3}$, which is an optimal condition for $2f_{ce}$ upper hybrid excitation. Another parameter is $\kappa_0 = ck_0/\Omega_e$ in equation (12), which we chose as $\kappa_0 = 4$. The final one is the spectral width parameter $\Delta = c\delta k/\Omega_e$. Of the latter two,

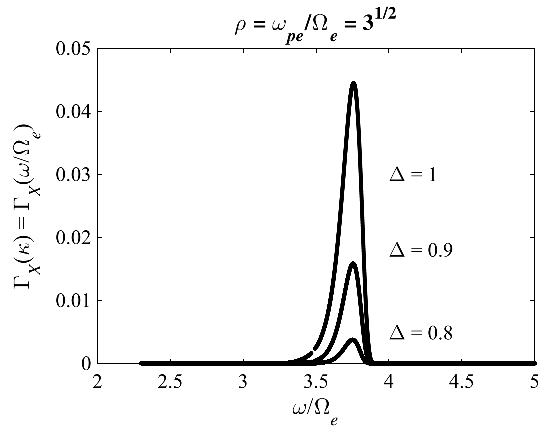

Figure 2. The normalized X mode nonlinear growth rate $\Gamma(\kappa) = \Gamma(\varpi)$ versus $\varpi = \sqrt{\varpi_R + \kappa^2}$ for $\rho = \sqrt{3}$, $\kappa_0 = 4$ and for three different values of spectral width parameter, $\Delta = 1$, 0.9, and 0.8.

we find that the nonlinear growth rate Γ_x (13) is very sensitive to the spectral width of the two upper hybrid (or Z) modes, namely, $\Delta = c\delta k/\Omega_e$, but not on $\kappa_0 = ck_0/\Omega_e$. To demonstrate the sensitive dependence of Γ_x on $\Delta = c\delta k/\Omega_e$, we plot in Figure 2 the dimensionless nonlinear growth rate Γ_X for three different values of Δ. The first case of $\Delta = 1$ is the same as in Figure 1. As we slightly reduce this parameter to $\Delta = 0.9$, one can see that the nonlinear growth rate decreases substantially. For another slight decrease, to $\Delta = 0.8$, the growth rate becomes very low in magnitude. This shows that the nonlinear generation of $4f_{ce}$ emission may indeed be restricted by the spectral property of the underlying $2f_{ce}$ upper hybrid modes, especially their spectral width in wave number space, which cannot be completely understood unless one solves not only the entire weak turbulence equation (1) but also the linear wave growth and damping equation. Such a task is the subject of future research.

From an observational point of view, although one does not measure $\Delta = c\delta k/\Omega_e$ directly, one may determine the frequency bandwidth, $\delta\omega$, by observation. If we approximately assume $\omega \sim kv_e$, where v_e is the characteristic speed for the electrons that interact to generate the upper hybrid waves, then we have $\delta\omega \sim \delta kv_e$, or combining with the definition, we have $\Delta = (\delta\omega/\Omega_e)(c/v_e)$. From Figure 5 of the companion paper *LaBelle and Chen* [2016], we have $\delta f \sim 0.1$ MHz and $f_{ce} \sim 1.25$ MHz, and so $\Delta > 1$ (the condition for efficient nonlinear wave generation) requires $v_e < c/12.5$, implying $E < 1.8$ keV. This calculation is interesting because there have been few previous estimates of the electron energies. Most estimates have suggested a somewhat higher energy, e.g., ~2.5–10 keV, based on in situ observations [*Gough and Urban*, 1983; *Samara et al.*, 2004], and previous theoretical work has assumed electron beams with those energies. Future more rigorous modeling efforts based on the theory presented above will be valuable to place constraints on the energy of the causative electron beam.

Some open theoretical questions and observational tests that remain outstanding are these: First, if $2f_{ce}$ roars can merge to produce $4f_{ce}$ right-hand/X mode roars, then why are not most, if not all, of observed $2f_{ce}$ roars accompanied by $4f_{ce}$ roars? Potential resolutions to this open question may be that the intensity of $2f_{ce}$ roars must be sufficiently high. If the intensity is not high enough, then the two induced decay terms ignored in equation (1) may no longer be ignorable. If these terms have opposite sign, then the decay instability might be suppressed. The wave intensity is related to the electron energy, which is tentatively estimated to be in the low keV range. A comprehensive theoretical model must be employed in order to test this issue.

Another possible aspect involves the spatial inhomogeneity. In order for $2f_{ce}$ roars to undergo decay instability, the rays associated with these electrostatic modes must be confined within a close vicinity. Otherwise, if the rays diverge away from the source region, then the wave-wave interaction may not become very efficient. To investigate this scenario, one must treat the problem not only as a spatially nonuniform system, but one must also consider the ray path propagation in spatially inhomogeneous domain.

An interesting observational test would be to see whether $3f_{ce}$ roars may be able to generate $6f_{ce}$ roars by nonlinear process discussed in the present paper, since our theory is equally applicable to such a situation.

Acknowledgments
The present paper does not involve any spacecraft data analysis. However, upon request, numerical data for generating all the figures will be made available. The research at the University of Maryland was supported by NSF grants AGS1147759 and AGS1550566. The research at Kyung Hee University was supported by the BK21-Plus grant from the National Research Foundation (NRF), Korea. P.H.Y. acknowledges the Science Award Grant from the GFT Foundation to the University of Maryland. The research at Dartmouth College was supported by NSF grants AGS-1147699 and PLR-1443338. The research at Merrimack College was supported by NSF grants PLR-1248062 and PLR-1443542.

References

Fung, S. F., and K. Papadopoulos (1987), The emission of narrow-band Jovian kilometric radiation, *J. Geophys. Res.*, *92*, 8579–8593, doi:10.1029/JA092iA08p08579.
Gough, M. P., and A. Urban (1983), Auroral beam/plasma interaction observed directly, *Planet. Space Sci.*, *31*, 875–883.
Kellogg, P. J., and S. J. Monson (1979), Radio emissions from the aurora, *Geophys. Res. Lett.*, *6*(4), 297–300, doi:10.1029/GL006i004p00297.
LaBelle, J. (2012), First observations of $5f_{ce}$ auroral roars, *Geophys. Res. Lett.*, *39*, L19106, doi:10.1029/2012GL053551.
LaBelle, J., and M. Dundek (2015), Comparison of fine structures of electron cyclotron harmonic emissions in aurora, *J. Geophys. Res. Space Physics*, *120*, 8861–8871, doi:10.1002/2015JA021631.

LaBelle, J., and Y. Chen (2016), 4f_{ce} auroral radio emissions 1. Observations, *J. Geophys. Res.*, *121*, doi:10.1002/2016JA022890, in press.

Melrose, D. B. (1991), Emission at cyclotron harmonics due to coalescence of *z*-mode waves, *Astrophys. J.*, *380*, 256–267, doi:10.1086/170582.

Roux, A., and R. Pellat (1979), Coherent generation of the auroral kilometric radiation by nonlinear beatings between electrostatic waves, *J. Geophys. Res.*, *84*, 5189–5198, doi:10.1029/JA084iA09p05189.

Samara, M., J. LaBelle, C. A. Kletzing, and S. R. Bounds (2004), Electrostatic upper hybrid waves where the upper hybrid frequency matches the electron cyclotron harmonic in the auroral ionosphere, *Geophys. Res. Lett.*, *31*, L22804, doi:10.1029/2004GL021043.

Sato, Y. T. O., M. Iizima, A. Kumamoto, N. Sato, A. Kadokura, and H. Miyaoka (2008), Auroral radio emission and absorption of medium frequency radio waves observed in Iceland, *Earth Planets Space*, *60*(3), 207–217.

Sato, Y., T. Ono, N. Sato, and R. Fujii (2010), MF/HF auroral radio emissions emanating from the topside ionosphere, *Geophys. Res. Lett.*, *37*, L14102, doi:10.1029/2010GL043731.

Sato, Y., T. Ono, N. Sato, and Y. Ogawa (2012), First observations of 4f_{ce} auroral roar emissions, *Geophys. Res. Lett.*, *39*, L07101, doi:10.1029/2012GL051205.

Sato, Y., A. Kadokura, Y. Ogawa, A. Kumamoto, and Y. Katoh (2015), Polarization observations of 4f_{ce} auroral roar emissions, *Geophys. Res. Lett.*, *42*, 249–255, doi:10.1002/2014GL062838.

Shepherd, S. G., J. LaBelle, and M. L. Trimpi (1997), The polarization of auroral roar emissions, *Geophys. Res. Lett.*, *24*(24), 3161–3164, doi:10.1029/97GL03160.

Vlahos, L., R. R. Sharma, and K. Papadopoulos (1983), Stochastic three-wave interaction in flaring solar loops, *Astrophys. J.*, *275*, 374–390, doi:10.1086/161540.

Weatherwax, A. T., J. LaBell, M. L. Trimpi, and R. Brittain (1993), Ground-based observations of radio emissions near 2f_{ce} and 3f_{ce} in the auroral zone, *Geophys. Res. Lett.*, *20*(14), 1447–1450, doi:10.1029/GL020i014p01447.

Willes, A. J., S. D. Bale, and Z. Kuncic (1998), A *z* mode electron-cyclotron maser model for bottomside ionospheric harmonic radio emissions, *J. Geophys. Res.*, *103*, 7017–7026, doi:10.1029/97JA03601.

Yoon, P. H., A. T. Weatherwax, and T. Rosenberg (1998), On the generation of auroral radio emissions at harmonics of the lower ionospheric electron cyclotron frequency: *X*, *O*, and *Z* mode maser calculations, *J. Geophys. Res.*, *103*(A3), 4071–4078, doi:10.1029/97JA03526.

Yoon, P. H. (2015), Kinetic theory of weak turbulence in magnetized plasmas: Perpendicular propagation, *Phys. Plasmas*, *22*, 082310, doi:10.1063/1.4928380.